

# Adsorption of Uranium from Sulfate Medium using Synthetic Polymer; Kinetic Characteristics



El-sheikh AS<sup>1\*</sup>, E A Haggag<sup>1</sup> and Abd El-Rahman NR<sup>2</sup>

<sup>1</sup>Nuclear Materials Authority, Cairo, Egypt

<sup>2</sup>Petrochemicals Department, Egyptian Petroleum Research Institute, Nasr City, Cairo, Egypt

Submission: August 08, 2019; Published: October 17, 2019

\*Corresponding author: El-sheikh AS, Nuclear Materials Authority, Cairo, Egypt

## Abstract

Polyurethane was prepared dodecyl amine (hydrogen donating group) reaction with toluene diisocyanate (TDI) to obtain the polyurethane polymer. The equilibrium and kinetic characteristics of the Polyurethane have been determined. The adsorption factors have been optimized. The adsorption capacity of uranium attained 70 mg/g that accords with Langmuir isotherm (75 mg/g). The adsorption process is follow pseudo second order reaction.

**Keywords:** Polyurethane manufacture; Uranium Adsorption; Synthetic Polymer, Kinetic Characteristics; Polyurethane; Organic Solvents

**Abbreviations:** PU: Polyurethane; SAPOs: Silicoaluminophosphates; TDI: Toluene Diisocyanate; GPC Gel Permeation Chromatography; PST: Standard Polystyrene; AC: Active Carbon; LLE: Liquid-Liquid Extraction; ECD: Electrochemical Deposition; CPE: Cloud-Point Extraction; SPE: Solid-Phase Extraction

## Introduction

PU (polyurethane) polymers are playing an imperative character in many activities because of their generally mechanical properties and their skill to be moderately easily machined and molded as plastics, foams and elastomers. Actually, urethane materials, such as foams and elastomers, have been established to be favorable for many applications. The manufacture of PU (polyurethane) includes the reaction of isocyanate groups (diisocyanate) and hydroxyl groups (polyol) leading to urethane groups. The second reaction is the gas manufacture that include the reaction of isocyanate groups with water to form a mine and CO<sub>2</sub> (chemical puffing cause) in the form of foams [1]. The PU (polyurethanes) are three types: flexible foams when the used polyols molecular weights greater than 2500 g/mole; semi-rigid foams used polyols with molecular weights of 2000-6000 g/mole; while rigid foams used littler chain polyols with molecular weights of 200 to 4000 g/mole [2]. PU (polyurethane) dispersions are polymer dispersions exhibit numerous benefits including the low instability in organic solvents, non-toxicity and non-flammability properties [3]. For this object, PU (polyurethane) dispersions gained detailed study and established to more environmental, recyclable and well-designed substrates [4]. Among all types of polyurethane dispersions, cationic polyurethanes are characterized by high resistivity near the hydrolytic effects of acid and alkali and can be used in the mixture of leather surfactant, dye dispersants and cloth dying agents [5].

Organic fatty acids are renewable, environmentally friendly and recyclable natural materials. The introduction of fatty acids, either clean acids or mixture of conformist fatty acids [6] into cationic PU (polyurethane) polymeric chains growths their eco-friendly goods. Additionally, the attained compounds are provided more potential purposes such as revolving the polymer chains to extra homogeneous by organic compounds. These types make cationic polyurethanes more industrially arresting fresh material in the polyurethane industry. Cationic polyurethane was synthesized by the reaction of Tung oil with polyurethane ingredients [7]. Cationic PU (polyurethane) surfactants had best dispersion, film-forming facility and permanence [8], environmental affability [9]. In this revision, a chain of cationic polymeric surfactants and their silver nanocomposite were organized. Their chemical structures were indomitable using changed analytical methods. The effect of the cationic polymeric chains on their surface properties was examined. Numerous separations and preconcentration techniques have been done for metal-ion, namely; cloud-point extraction (CPE) [10,11], co-precipitation [12], electrochemical deposition (ECD) [13], Flotation [14], liquid-liquid extraction (LLE) [15], solid-phase extraction (SPE) [16-18], solid-phase microextraction (SPME) [19]. However, SPE is the preferred method mainly due to its simplicity, direct application in microliter (IL) volume, fastness, minimal sample loss, higher preconcentration factor, rapid phase separation, cost and time saving [20].

The SPE method is based on the principle of analyte transfer from the aqueous medium, phase, to the active sites on the solid phase of an adsorbent [21]. A lot of adsorbents have been applied for metal ions, including alumina [22,23], activated carbon (AC) [24-27], C18 cartridge silica, chelex-100 [28], polyurethane foam [29], microcrystalline naphthalene [15,17], silica gel [30], nanoparticles [31,32], cyclodextrins CDs [33], zeolites [34] and clay [35]. Adsorption is a mass transfer process from liquid or gas to solid phase. In order to enhance adsorption efficiency, this solid surface should be porous and should have high specific area. In recent years, utilizing low price adsorbents has become common. Some of these adsorbents are waste industrial materials which have suitable functional groups for reacting with metal. Crab shell, papaya wood, Indian bamboo, cotton, natural zeolites, fish scale and etc. are typical natural adsorbents useful for removing heavy metals [35]. The synthetic zeolites such as Silicoaluminophosphates (SAPOs) or some polymeric adsorbents could be noted as synthetic adsorbents used in this area. PUs has various applications as different forms such as soft and hard foams, elastomers, thermoplastics elastomers, resin, dye, covering and etc. all around the world. One of the vital applications of this polymer is at adsorption process. Since this polymer comprises amide functional groups, it could be used as industrial adsorbent. Cu ion has been removed from contaminated water solutions by 2-Mercapto-benzothiazole modified polyurethane foam. The continuous experiments have been done through preparing adsorption columns for studying and optimizing the effect of primary concentration of the metal, pH, adsorbents used in respect of gram and various conditions for preparing the used polyurethane [36]. The prepared composite material showed less binding time with metal

ions, great affinity and high enrichment. Cd (II), Cr (III), and Pb (II) extraction has been studied using SPE extraction method. The parameters that influence the sorption, extraction and elution efficiency of the metal ions were also studied [37].

## Experimental

### Chemicals and Reagents

The standard uranium sulfate solution was prepared by dissolving an appropriate amount of uranyl sulfate trihydrate  $UO_2SO_4 \cdot 3H_2O$  from Blabs, Florida, USA. Toluene diisocyanate (TDI), Dodecyl amine, acetyl chloride were systematic rank chemicals delivered from Sigma Aldrich, Germany.

### Synthesis of Polyurethane Sorbent

Triethanol amine esters palmitate (0.20 mol) and toluene diisocyanate (0.10 mol) were liquefied in 2-butanone (80 mL) and reacted in 500 mL one necked flask under reflux condition. Temperature then has been increased slowly and stabilized at 140 °C for 24 h. Next that, the reaction medium is permitted to cooled to room temperature, however 2-butanone was exposed off for one day of introduction under reduced pressure (1/3 atm.) at 40 °C [38,39]. The produced polyurethane was washed twice by ethanol and withered in heartfelt oven for whole dehydration. The found polyurethanes were nominated as: PUP and PUS for palmitate and stearate. Molecular weight of the found polyurethanes were indomitable using HP 5890 gas chromatography provided with aflame ionization detector, and the average molecular weights of the changed polyurethanes were 2650 and 2830 g/mole for PUP (Figure 1) shows schematic diagram for preparing of the sorbent.

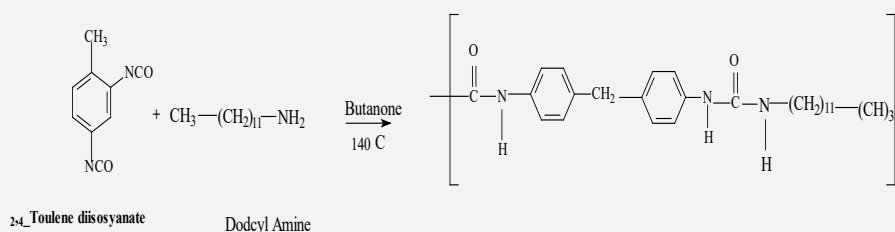


Figure 1: Synthesis of polyurethane polymeric chains.

**Gel permeation chromatography (GPC):** The molecular weight of the prepared polyurethane was indomitable using HP 5890 gas chromatography provided with a flame ionization detector, and the average molecular weight. of the prepared polyurethane was 3350 g/mole for PUA. GPC analysis of the specimens were achieved the conditions 0.80 ml/ min flow rate at 25°C in tetra hydro furan (THF) by using a Waters 150 component system (IR detectors) equipped with ultra-u-stragel columns (10 nm and 1000 nm) after calibrated with standard polystyrene (PSt).

### Uranium Adsorption Equilibrium Studies from sulfate Solution

The polyurethane sorbent was used for uranium extraction from sulfate solution by batch experiment. In this manner, a fixed

weight of PU (0.1g) contacted with (10 mL) uranium synthetic solution of 600 mg/L for known period at ambient temperature. Uranium concentration was measured before and after experiment. The adsorption efficiency was calculated according to relation (1):

$$U \text{ adsorption efficiency } \% = \frac{C_o - C_e}{C_o} \times 100 \quad \dots\dots (1)$$

Where  $C_o$  and  $C_e$  are the initial and equilibrium uranium concentration in solution (mg/L), respectively. Calculation of uranium adsorption quantity  $q_e$  (mg/g) has been carried at the equilibrium time according to relation 2

$$q_e = (C_o - C_e) \times \frac{V}{m} \quad \dots\dots\dots (2)$$

Where  $V$  is the volume of solution (L),  $m$  is the weight of the

resin (g). The distribution coefficient ( $K_d$ ) of uranium between the aqueous bulk phase and the solid phase was calculated from the following relation (3):

$$K_d = \frac{C_o - C_e}{C_e} \times \frac{V}{m} \dots\dots\dots (3)$$

**Equilibration Calculation:** All uranium speciation was done with a chemical equilibrium calculation program [39]

**Control Analysis**

Uranium analysis was determined spectrophotometrically using Arzenazo III at 655 nm [40]. In the meantime, this analysis was confirmed by the oxidimetric volumetric determination of

uranium using ammonium metavanadate. This procedure is based on the titration of U+4 with ammonium vanadate  $NH_4VO_3$ ; namely



**Results and Discussion**

**Uranium Adsorption from sulfate solution using polyurethane sorbent**

The factors that affect the uranium sorption efficiency from sulfate solution using solid-liquid batch technique were studied. The relevant factors include pH, Contact Time, temperature and Initial Uranium Concentration.

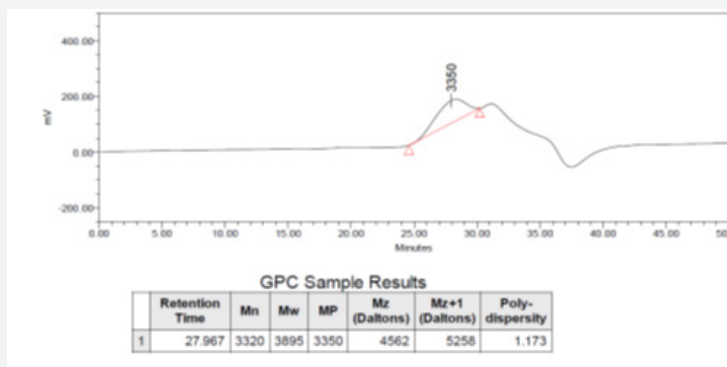


Figure 2: GPC Molecular weight detection for prepared PUA.

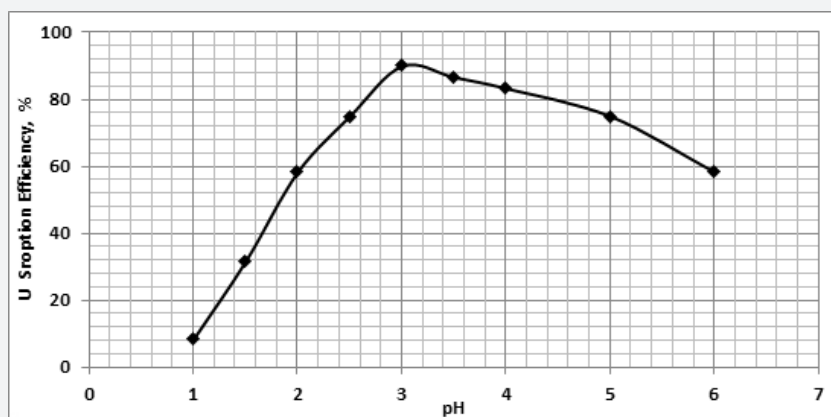
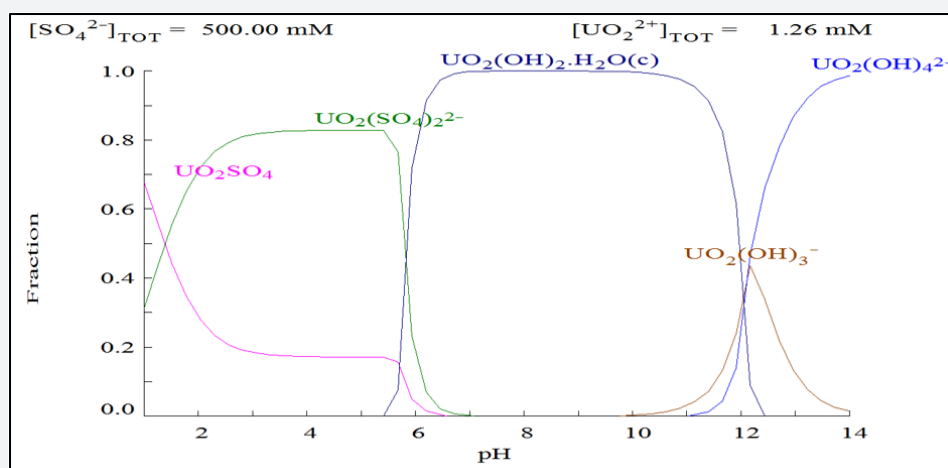


Figure 3: Sorption capacity of U(VI) as a function of equilibrium pH using PU sorbent (C0: 600 ± 5 mg L-1; contact time: 60 min; T:25 ± 1 °C).

**Effect of pH:** The effect of pH on uranium adsorption from polyurethane sorbent from sulfate solution was studied by contacting (0.1g) of PU with (10 mL) uranium synthetic solution of 600 mg/L at 25 °C for 60 minutes. The examined pH ranged from 1.0 to 6.0. The achieved data were presented in (Figure 2). From the obtained results, it could be concluded that the maximum uranium adsorption was achieved at pH between 2.5 and 3.5 was 90 % adsorption efficiency. This is due to the anion complexes of uranium ( $UO_2(SO_4)_2^{2-}$ ). Accordingly, pH 2.5-3.5 was the best range and consequently, pH 3 was selected for the subsequent experiments. / (Figure 3) Sorption capacity of U(VI) as a function of equilibrium pH using PU sorbent (C0: 600 ± 5 mg L-1; contact time: 60 min;

T:25 ± 1 °C) The aqueous speciation distribution of uranium was calculated and represented in (Figure 3). The results showed that the complexes of  $UO_2SO_4$  and  $UO_2(SO_4)_2^{2-}$  were the predominant species at the pH range from 0.0 – 5.5 with a mean total percent of 8.33 and 75% respectively, whereas it was 18 and 82 % at pH 5.5. U-hydroxide complexes start to dominate the aqueous phase at pH near 6. The dominate complex of  $UO_2(OH)_2 \cdot H_2O$  became the major species with about 100% of total concentration at pH range from 6 to 12. After pH 12,  $UO_2(OH)_4^{2-}$  and  $UO_2OH^{3-}$  became the major species. Expected aqueous speciation of uranium (600 mg/L) as a function of pH in 0.5 M  $H_2SO_4$  using Medusa and Hydra program (Figure 4).



**Figure 4:** Expected aqueous speciation of uranium (600 mg/L) as a function of pH in 0.5 M H<sub>2</sub>SO<sub>4</sub> using Medusa and Hydra program.

**Effect of Contact Time:** The impact of the contact time was studied using weight of PU was (0.1g) with a uranium solution (10 ml) having a concentration of 600 mg/L and pH 3 at temperature (25, 35, 45, 55 and 65 °C). / Figure 5 Effect of contact time upon the uranium adsorption efficiency on the PU (PU weight = 0.1 g, volume = 10 ml, pH = 3, U conc.= 600 mg/L) The studied time ranged from 2.5 to 120 minutes. The results were plotted in (Figure 4). The studied time ranged from 2.5 to 120 minutes. The

reached results were plotted in (Figure 4). It was detected that the uranium adsorption efficiency attained about 83.33% for 60 minutes contact time at temperature 25 °C while it reached to 93.33% at 65 °C. By increasing the contact time from 60 to 120 minutes, the uranium adsorption efficiency attained about 90.0% for 120 minutes contact time at temperature 25 °C while it reached to 96.6% at 65 °C. Therefore, 120 min. is selected as the suitable contact time.

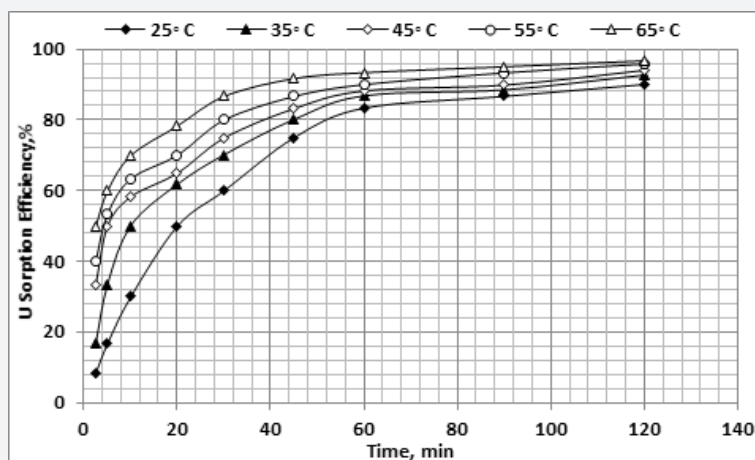


**Figure 5:** Effect of contact time upon the uranium adsorption efficiency on the PU (PU weight = 0.1 g, volume = 10 ml, pH = 3, U conc.= 600 mg/L).

**Effect of adsorption temperature:** The influence of adsorption temperature explored by contacting fixed portions 0.1g of PU with 10 ml of 600 mg/L uranium. The other factors were fixed at a contact time of 120 min, and solution pH of 3.0. Several studies were carried out at a series of temperatures from 25 to 65 °C. The experimental results are plotted in (Figure 6) as a relation between uranium adsorption efficiency and temperature. The obtained results show that, the uranium adsorption efficiency slightly increases with increasing temperature. The increase of uranium sorption at higher temperature may be due to the increase in the activation of the sorbent surface. As the adsorption efficiency was not distinguished, there is no need to control or alter the temperature.

**Effect of Initial Uranium Concentration:** To inspect the effect of initial uranium concentration upon its adsorption efficiency onto PU, a series of experiments were performed by contacting a fixed weight (0.1 g) of the studied PU with 10 ml of 600 mg/L uranium concentration and pH 3 for 120 min at room temperature (25°C). The studied initial uranium concentrations ranged from 100 up to 1200 mg/L. The obtained results were plotted in (Figure 7). From the obtained data, it was found that, the adsorption efficiency is inversely proportional to its initial concentration. In contrast, the adsorption capacity is directly proportional to initial uranium concentration till stabilization after 800 mg/L where at this point experimental adsorption capacity of the adsorbent was about 70 mg uranium/g PU.

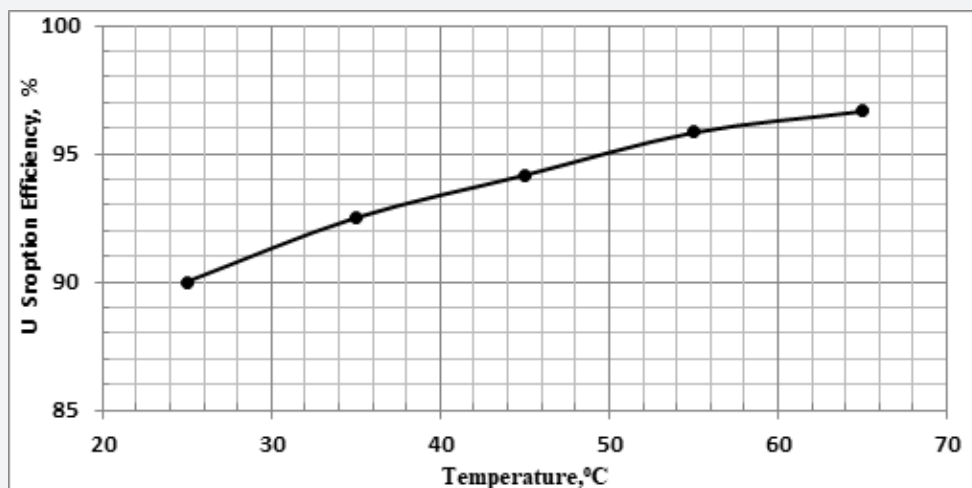


Figure 6: Effect of temperature on uranium adsorption efficiency onto PU (PU weight = 0.1 g, volume = 10 ml, pH = 3, U conc.= 600 mg/L).

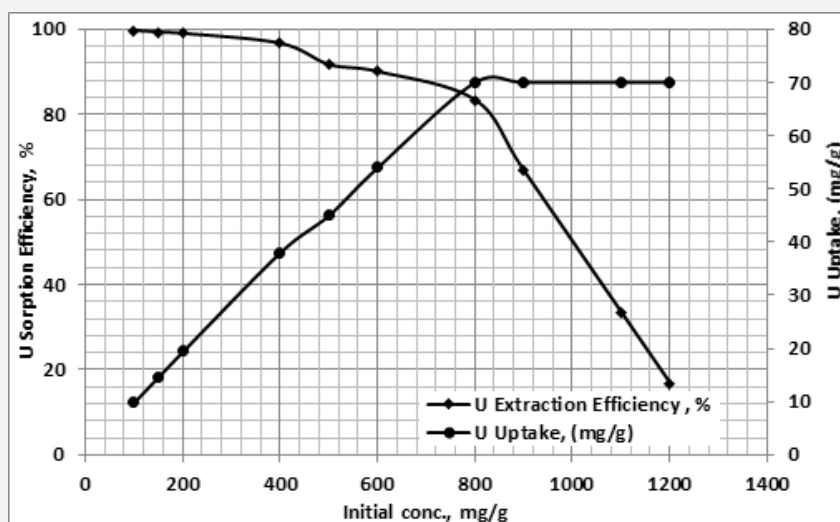


Figure 7: Effect of initial uranium concentrations on uranium adsorption efficiency and uranium uptake (PU weight = 0.1 g, volume = 10 ml, pH=3, 120 min, 25 °C).

**Adsorption Isotherm:** A number of common adsorption isotherm models were considered to fit the attained isotherm data under the equilibrium adsorption of the PU. Examples of these models are Langmuir and Freundlich.

**A. Langmuir Isotherm:** Langmuir model suppose that, the adsorption occurs uniformly on the active sites of the sorbent, and once a sorbate occupies a site, no further sorption can take place at this site [41-43].

Table 1: Langmuir and Freundlich parameters for uranium adsorption onto PU.

Langmuir model parameters			Freundlich model parameters			
$q_{max}$ (mg/g)	$KL$	$R^2$	$K_f$ (mg/g)	$n$	$R^2$	
76.33	0.028	0.999	4.967	2.17	0.841	

Langmuir model is given by the following equation:

$$\frac{C_e}{q_e} = \frac{C_e}{q_{max}} + \frac{1}{KLq_{max}} \dots\dots (4)$$

Where  $KL$  is a constant of the adsorption equilibrium (L/mg),  $q_{max}$  is the saturated monolayer adsorption capacity (mg/g) while  $q_e$  and  $C_e$  are the uranium uptake capacity (mg/g) of adsorbent and the residual uranium concentration (mg/L) at equilibrium respectively. A linearized plot of  $C_e/q_e$  against  $C_e$  gives  $q_{max}$  and  $KL$  as shown in (Figure 8). The Langmuir parameters are given in (Table 1). Langmuir model is thus suitable for the de-

scription of the adsorption equilibrium of uranium onto material composite. Langmuir model is thus suitable for the description of the adsorption equilibrium of uranium onto material composite. The essential characteristics of the Langmuir isotherm can be expressed in terms of a dimensionless constant separation factor,  $R_L$ , which is used to predict if an adsorption system is favorable or not. The separation factor,  $R_L$ , is given by the following Eq. (5):

$$R_L = \frac{1}{1 + K_L C_o} \dots\dots (5)$$

Where  $C_o$  is the initial uranium (VI) concentration (mg/L) and

$K_L$  is the Langmuir adsorption constant (L/mg). The calculated  $R_L$  value for uranium (VI) concentration of 600 mg U/L is  $2.18 \times 10^{-5}$  which was in the range of 0.0 to 1.0 and indicates that the adsorption of uranium (VI) on PU material is favorable [44-47].

**B. Freundlich Isotherm:** The Freundlich model stated that the ratio of solute adsorbed to the solute concentration is a function of the solution. The empirical model was shown to be consistent with exponential distribution of active centers, charac-

**Table 2:** The experimental capacity of PU compared with the adsorption capacity of some resins and different modified polymers.

Type	Adsorption Capacity (mg/g)	Ref.
polyethyl eniminephenyl phosphonamidic acid	39.66	[44]
N-dimethyl-N, N-dibutyl malonamide functionalized polymer	18.78	[45]
succinic acid impregnated amberlite XAD-4	12.33	[46]
gel-amide	28.98	[47]
gel-benzamide	18.64	[47]
natural clinoptilolite zeolite	0.7	[48]
Lewatit TP 214	81.75	[49]
Lewatit TP 208	308.65	[49]
4-(2-Pyridylazo) resorcinol (PAR), Amberlite XAD-16	115.5	[50]
Polyurethane polymer	76.33	Present work

teristic of heterogeneous surfaces [41-43]. The amount of solute adsorbed at equilibrium,  $q_e$ , is related to the concentration of solute in the solution,  $C_e$ , by the following

$$q_e = K_f C_e^{1/n} \quad (6)$$

This expression can be linearized to give:

$$\log q_e = \log K_f + \frac{1}{n} \log C_e \quad (7)$$

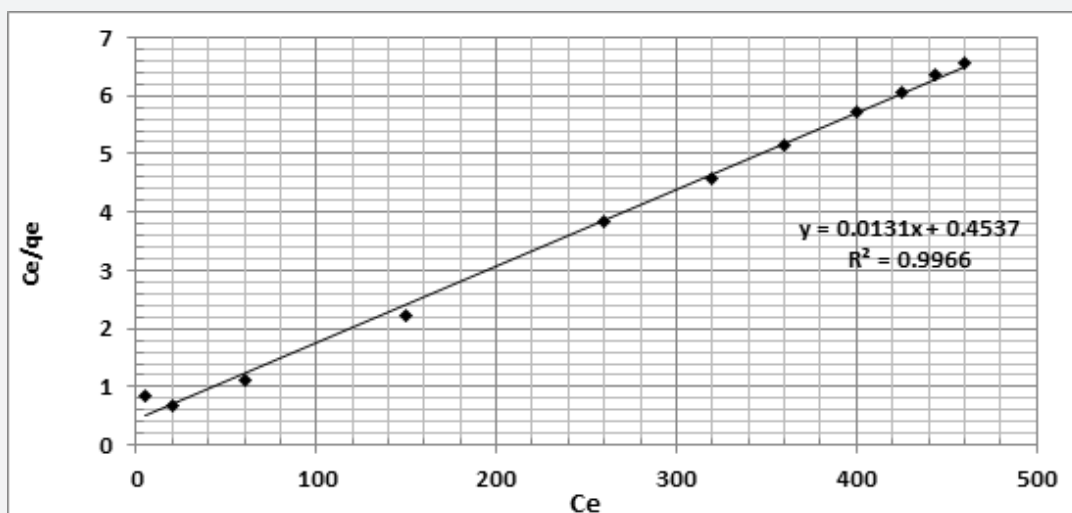


**Figure 8:** Langmuir isotherm plot for adsorption of uranium onto PU.

Where  $K_f$  and  $n$  are the Freundlich constants, which represent sorption capacity and sorption intensity, respectively. A plot of  $(\log q_e)$  versus  $(\log C_e)$  would result in a straight line with a slope of  $(1/n)$  and intercept of  $(\log K_f)$  as seen in (Figure 9) Freundlich constants are given in (Table 1). By comparing the isotherms applied with the experimental results, Langmuir gave the best fit, while Freundlich isotherm did not fit well. A comparison of the adsorption capacity of PU with some other sorbents is provided in (Table 2).

**Effect of phase ratio (S/L):** The effect of dose concentration (S/L) from 0.1/1 to 0.1/50 which R is polyurethane polymer and S is aqueous was studied under the conditions of uranium initial concentration of 800 mg/L, pH of 3.0 at ambient temperature for 120 minutes. The result of uranium equilibrium exchange capaci-

ty for the polyurethane polymer was graphically plotted in (Figure 10). The results revealed that the uranium adsorption increases gradually by decreasing the S/L ratio from 0.1/1 to 0.1/50 for the polyurethane polymer without further increase. As a result, the polyurethane polymer/aqueous ratio of 0.1/25 were the more favorable ratio for the polyurethane polymer [48-50].

**Characterization of the synthesized sorbent**

**Fourier Transform Infrared (FTIR):** FT-IR spectroscopy was employed to demonstrate the interactions between PU and U (VI) ions. The spectra of PU before and after loading with U (VI) ions were presented in (Figure 11). The FT-IR spectrums of the studied PU and U (VI) loaded resin exhibited several peaks. The peak around  $3320 \text{ cm}^{-1}$  for strong band of the N-H stretching vi-

brations was observed for both situations. On the lower frequency side of this band at about  $2923\text{cm}^{-1}$  related to the stretching vibrations of the ring C-H bands of the polyurethane (cross-linked polyurethane). The peaks were found at  $1720\text{ cm}^{-1}$  (C=O stretching of secondary amide bonds),  $1635\text{ cm}^{-1}$  (C=C stretching of skeletal vibration of aromatic ring),  $1569\text{ cm}^{-1}$  (N-H bending vibrations of  $1^\circ$  amine). The ring C-C stretching and the scissoring of the methylene groups (bending  $-\text{CH}_2$ ) appeared at  $1468\text{ cm}^{-1}$  and

$1376\text{ cm}^{-1}$  (Vinyl and Vinylidene of C-H in-plane bend). After the adsorption, the intensity of some bands changed, and transmittance of peaks was relatively greater in the case of PU loaded with U(VI) ions compared to the PU. After adsorption, the most bands were shifted from  $5\text{ cm}^{-1}$ , that provided evidence of the interaction between U(VI) and PU as uranyl ion complex. The new peaks  $1161\text{ cm}^{-1}$  and  $925\text{ cm}^{-1}$  appeared after adsorption U(VI) was observed suggesting the uptake of U(VI) by PU [51].

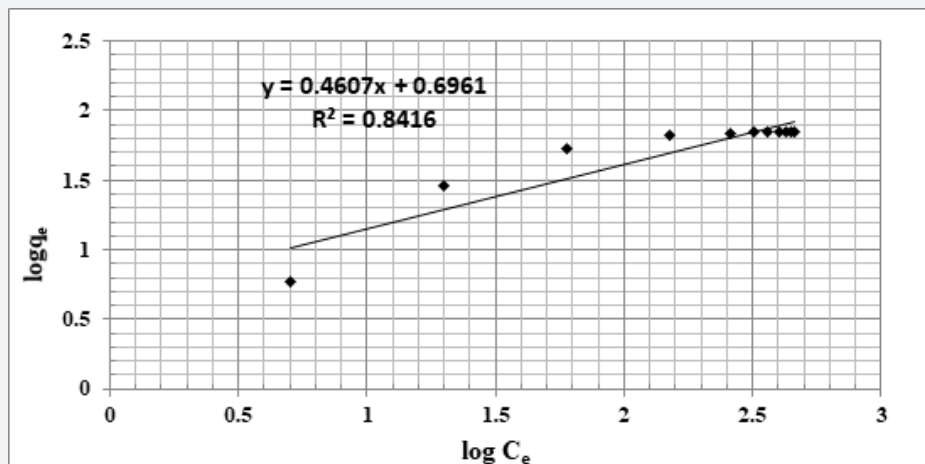


Figure 9: Freundlich isotherm plot for adsorption of uranium onto PU.

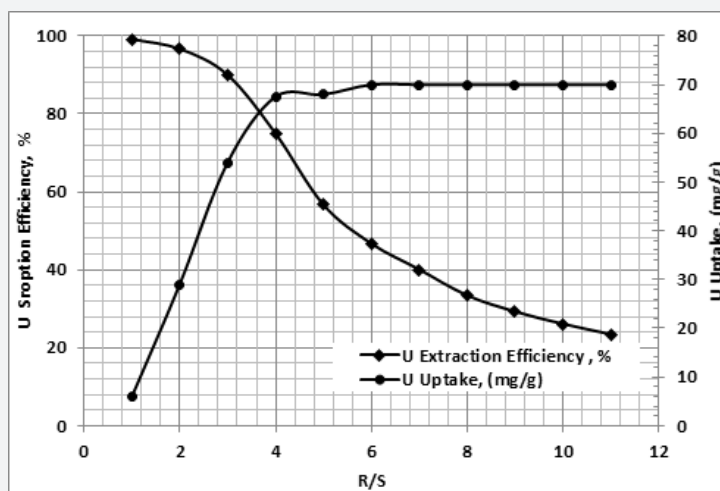


Figure 10: Effect of adsorbent dose upon uranium adsorption efficiency onto PU (PU weight = 0.1 g, pH=3, 120 min, 25 °C).

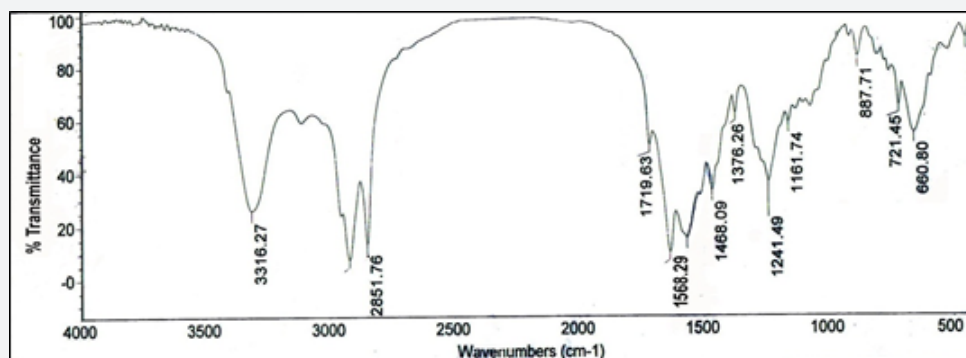


Figure 11: FT-IR spectrum of PU (A) before and (B) after uranium adsorption.

**Scanning Electron Microscope (SEM):** Scanning electron microscope (SEM) analysis is an important tool used in the determination of the surface morphology of an adsorbent. In this study, SEM has been utilized to detect the change in polyurethane morphological features before and after the adsorption process (Figure 12 A and B). The SEM results showed that the surface morphology of polyurethane after adsorption process is different from that of the surface before U(VI) adsorption. The polyurethane showed loose aggregates with a porous structure. After adsorption, the surface of polyurethane demonstrates compacted aggregates. The surface morphology of the polyurethane changed interface occurred during the experiment. As can be seen from the results, a visible change of the surface morphology in the U(VI) adsorbed demonstrated that the sorption of U(VI) had taken place onto the polyurethane sorbent.

**Adsorption Kinetics and Mechanism:** The data obtained

from batch experiments which were performed at different temperatures (25–65) °C were evaluated by using the simple Lagergren equation [52] to determine the rate of the sorptive interactions assuming pseudo first order kinetics. Thus, the Langmuir model is given by the relation (8):

$$\text{Log}(q_e - q_t) = \text{Log}q_e - \left(\frac{K_1}{2.303}\right)t \dots\dots\dots (8)$$

where  $q_t$  and  $q_e$  are the amounts of uranium adsorbed (mg/g) at time,  $t$  (min) and equilibrium time (90 min), respectively and  $K_1$  is the pseudo first order Lagergren adsorption rate constant ( $\text{min}^{-1}$ ). The  $K_1$  values could be obtained by plotting  $\log(q_e - q_t)$  versus  $t$  for adsorption of uranium at different temperatures as shown in (Figure 13). The values of the first order rate constant ( $K_1$ ) and correlation coefficient ( $R^2$ ) obtained from these plots are listed in (Table 3). The values of  $K_1$  indicate that the rate of the process increases with temperature.

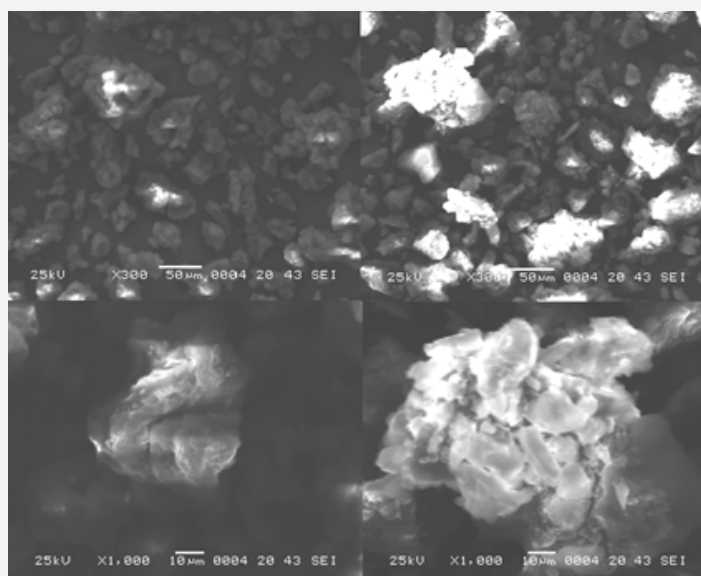


Figure 12: SEM micrographs of PU (A) before and (B) after uranium adsorption.

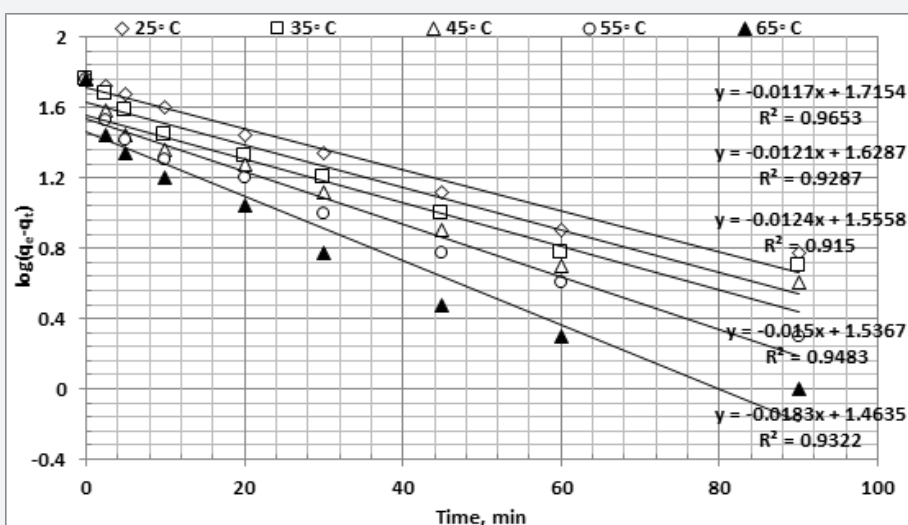


Figure 13: Lagergren plots for the adsorption of uranium (PU weight = 0.1 g, volume = 10 ml, pH 3, U Conc. = 600 mg/L).

**Table 3:** Data of kinetic parameters for uranium adsorption onto LMP resin.

°C	Lagergren pseudo first-order			R <sup>2</sup>	pseudo second order			
	K <sup>1</sup> (min <sup>-1</sup> )	q <sub>ecal</sub> (mg/ g)	q <sub>eexp</sub> (mg/ g)		K <sub>2</sub> (min <sup>-1</sup> )	q <sub>ecal</sub> (mg/ g)	q <sub>eexp</sub> (mg/ g)	R <sup>2</sup>
25	0.027	29.073	54	0.932	0.0009	60.82	54	0.982
35	0.0279	34.411	55.5	0.948	0.001	58.44	55.5	0.996
45	0.0285	35.958	56.5	0.915	0.002	58.18	56.5	0.997
55	0.0345	42.53	57.5	0.928	0.003	58.95	57.5	0.998
65	0.0422	51.927	58	0.965	0.005	59	58	0.999

The first order mechanism suffered from inadequacies when applied to uranium sorption on the PU. The pseudo first order plots in comparison with the experimental q<sub>e</sub> values are seen in (Table 3). The experimental q<sub>e</sub> values differed from the corresponding theoretical values. Thus, the interaction of uranium with the PU does not follow the first order kinetics. In order to ensure

the description of the kinetics, second order kinetic equation was applied which can be represented by the following linear equation [53]:

$$\frac{t}{q_t} = \frac{1}{K_2 \cdot q_e^2} + \left(\frac{1}{q_e}\right)t \dots\dots\dots (9)$$

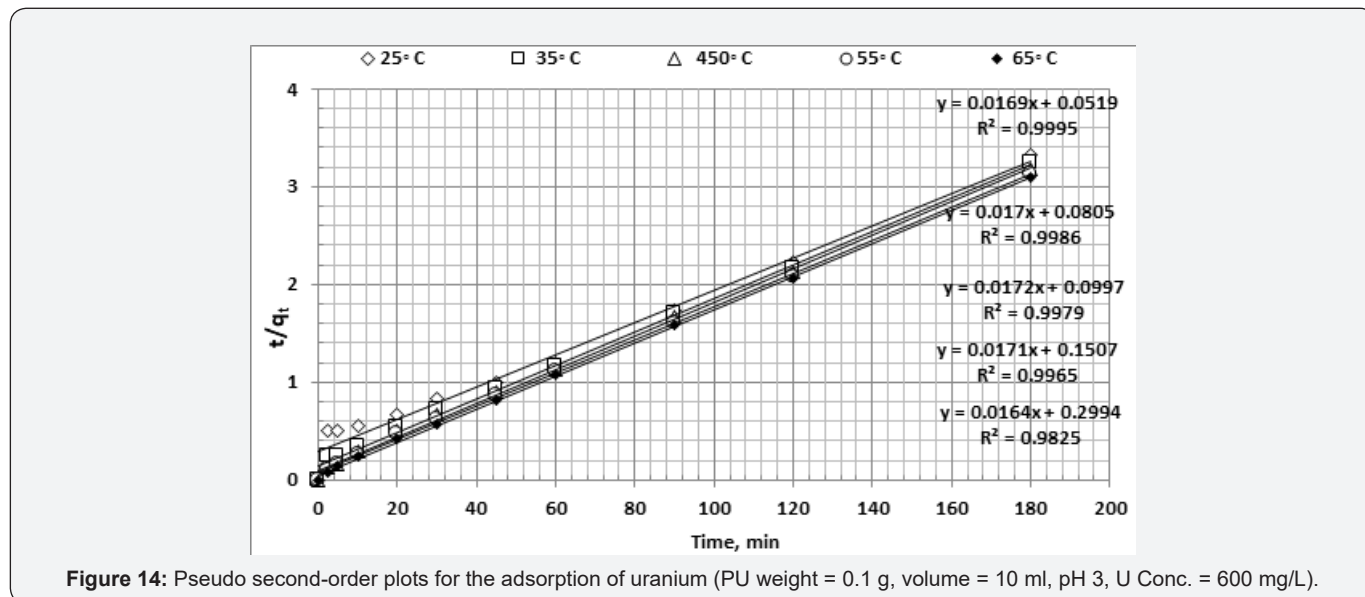


**Figure 14:** Pseudo second-order plots for the adsorption of uranium (PU weight = 0.1 g, volume = 10 ml, pH 3, U Conc. = 600 mg/L).

where K<sub>2</sub> is the second order rate constant (g. mg<sup>-1</sup> min<sup>-1</sup>). The kinetic plots of t/qt versus t for uranium are shown in (Figure 14). The plots show straight lines with good linearity temperatures. For the pseudo second order kinetic model, the correlation coefficients are closer to unity. The calculated equilibrium adsorption capacity (q<sub>e</sub>) is matches with the experimental data. The K<sub>2</sub> values show the applicability of the above equation for the resin. The values of the second order rate constant (K<sub>2</sub>) and correlation coefficient (R<sup>2</sup>) obtained from these plots are listed in (Table 3). Therefore, the sorption reaction are followed by the pseudo second order sorption more favorable as the predominant mechanism.

**Thermodynamic Characteristics:** The thermodynamic parameters of the studied adsorption process have been determined for uranium adsorption upon polyurethane polymer. Series of experiments were carried out at various temperatures ranging from 25 to 65 °C. These parameters were calculated for this system using the following Van't Hoff equation:

$$\ln K_d = \frac{\Delta S}{R} - \frac{\Delta H}{RT} \quad (10)$$

where K<sub>d</sub> (ml/g), ΔH (KJ/mol), ΔS (J/mol. K), T (Kelvin) and R (KJ/K.mol) are the distribution coefficient, the enthalpy, the entropy, the temperature in Kelvin and the molar gas constant respectively. The plotting of log K<sub>d</sub> against 1/T for uranium adsorption is shown in (Figure 15). The values of ΔH and ΔS were obtained from the slope and intercept of the latter plot while the Gibbs free energy, ΔG (KJ/mol), is calculated from the following equation:

$$\Delta G = \Delta H - T\Delta S \quad (11)$$

The calculated values of the thermodynamic parameters for U(VI)adsorption on polyurethane polymer are given in (Table 4). It was found that the enthalpy change (ΔH) and the entropy change (ΔG) were calculated to be 24.11 KJ/mol ad -0.417 KJ/mol respectively. Thus, the adsorption process was found to be endothermic and spontaneous. Results shown that value of S is positive

which means an increase in the randomness at the solid/solution interface during the sorption of the metal ion onto the sorbent, while the negative free energy value, indicating that uranium adsorption process is more favorable at high temperatures.

**Table 4:** Thermodynamic data for sorption of uranium ions onto polyurethane polymer.

$\Delta H$ KJ/mol	$\Delta S$ J/mol. K	$\Delta G$ KJ/mol
24.11±0.04	82.3±0.03	-0.417±0.01

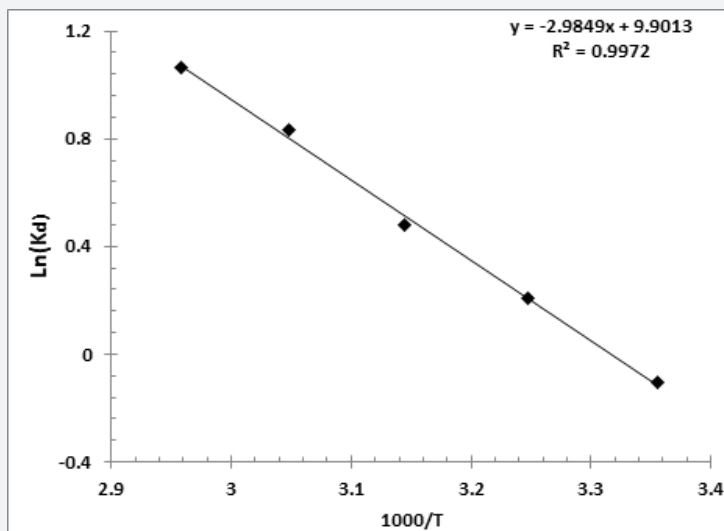


**Figure 15:** Plot of  $\ln K_d$  versus  $1/T$  of uranium ions onto polyurethane polymer.

### Uranium Elution

In order to achieve good metal elution from the composite material, number of stripping testes were carried out to elute the uranium ion from the loaded polymer after sorption process by using different solutions such as HCl,  $H_2SO_4$ ,  $HNO_3$ , NaOH,  $Na_2CO_3$ , NaCl,  $Na_2SO_4$ , and  $CH_3COONa$  to obtain the maximum stripping percent. Metal stripping experiments were performed using batch method at room temperature. The stripping experiments were carried out by shaking 0.1g loaded resin and 10 ml of 1 molar for

eluting reagent for 1 hour at 250 rpm. The result of uranium stripping from the composite material by using different solution was graphically plotted in (Figure 16). From the obtained result, it is clearly obvious that,  $HNO_3$  is the best eluent with 96% stripping efficiency.

**Precipitation of uranium:** Uranium precipitated from acidic solutions with hydrogen peroxide as shown in the following Equation 13.

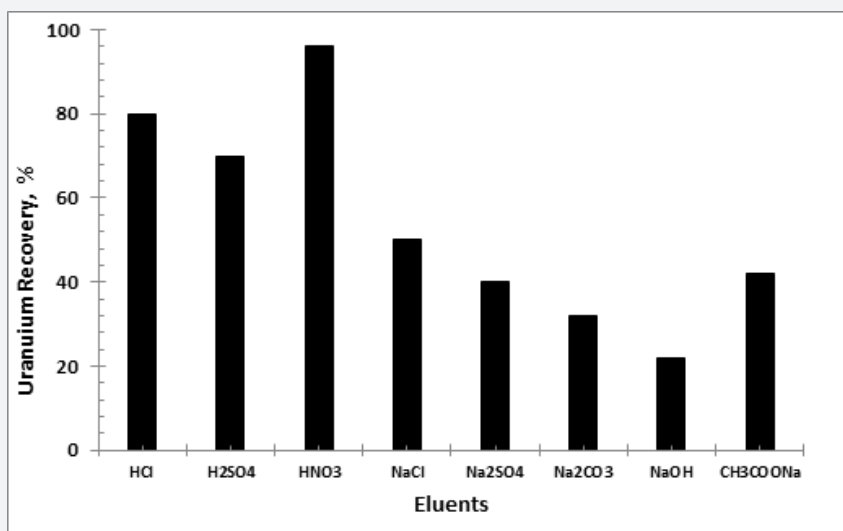
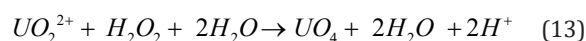


**Figure 16:** effect of different eluents on recovery of uranium.

Hydrogen peroxide was added in excess of the stoichiometric ratio at a temperature of about 25°C and a pH value of 2. Diluted sodium hydroxide was added to maintain the desired pH value. The solution was kept under mechanical agitation and the pH maintained until the end of the test. Precipitation was allowed to take place for 4 h and then the product was filtered out. The precipitate was dried at 110–120 °C for 48 hr. To reveal the structure of the precipitated uranium salt after elution, it was subjected to

x-ray diffraction analysis using Philips Pw 3710/31 diffractometer equipped with a scintillation counter. Measurement was made using Cu-target and Ni filter at 40 kV and 40 m A. From the obtained results shown in (Figure 17) and (Table 5), it is quite clear that the prepared sample matches with the structure Studtite (uranyl peroxide hydrate) with chemical formula  $UO_4 \cdot 4H_2O$  (ASTM card No. 49-1821).

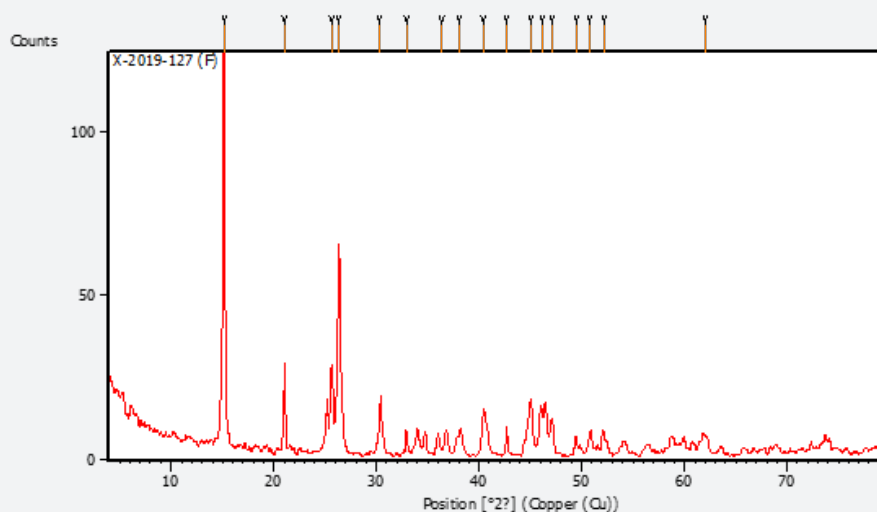


Figure 17: XRD spectra of the precipitated uranium after elution.

Table 5: X-ray Diffraction Data of the precipitated uranium after elution.

Pos. [°2θ]	Height [cts]	FWHM Left [°2θ]	d-spacing [Å]	Rel. Int. [%]	h	K	l
15.1649	109.21	0.2362	5.84251	100			
21.0372	26.45	0.1181	4.22304	24.22			
25.6086	26.57	0.2362	3.47862	24.33			
26.295	63.14	0.2755	3.38935	57.82			
30.3036	14.06	0.2755	2.94951	12.87			
32.9139	6.07	0.2362	2.72132	5.56			
36.3538	2.47	0.6298	2.47133	2.27			
38.125	6.76	0.7872	2.36049	6.19			
40.4632	13.72	0.3936	2.22933	12.57			
42.7206	8.59	0.2362	2.11661	7.86			
45.0776	16.84	0.4723	2.01127	15.42			
46.2308	12.49	0.4723	1.96375	11.44			
47.1506	10.84	0.3149	1.92756	9.92			
49.4698	5.54	0.3149	1.8425	5.07			
50.8195	6.92	0.4723	1.79668	6.34			
52.2349	5.74	0.4723	1.75128	5.25			
62.056	4.37	0.6298	1.49564	4.01			

### Reusability of the PU

The consistency of the obtained data on subsequent usage was confirmed by equilibrating 1.0 g of PU sample with uranium solution of 600 mg/L under the optimized experimental condi-

tions. The elution was carried out by using eluent agent of 1M  $HNO_3$  and the uranium concentration in each cycle was assessed. The results obtained on the subsequent usage of the same PU sample showed reproducible results with R.S.D. (Relative standa-

rad deviation) values about 1% up to 20 cycles. The obtained data is reflecting the reusability of PU. Therefore, it would be possible to reuse the working composite material for about 20 cycles without any noticeable loss of the adsorption capacity indicating that the developed composite material matrix has an adequately high mechanical stability in a manner to be recycled for 20 times.

## Conclusion

The batch tests which were performed to optimize the uranium adsorption by PU indicate that 70 mg U/g resin maximum saturation capacity was attained by adjusting the pH at 3 for 120 minutes contact time and with PU to Liquor ratio of 0.1/25 at ambient temperature. By applying Lagergren equation, the sorption reaction is more favorably to be pseudo-second order sorption, this is due to that the predominate mechanism and the values of  $K_2$  "second order rate constant" indicate that the rate of the process decreases with increasing temperature. Langmuir isotherm model is suitable for the description of the adsorption equilibrium of uranium onto PU, the calculated dimensionless constant separation factor " $R_L$ " value is too small which indicates that the adsorption of uranium on PU is favorable. From the thermodynamic parameters, a positive value of  $\Delta H$  shows that uranium adsorption is of an endothermic nature and the positive  $\Delta S$  parameter suggests increasing the system randomness at the solid-liquid interface during the adsorption process.

## References

- Chang LC, Xue Y, Hsieh FH (2001) Comparative study of physical properties of water blown rigid polyurethane foams extended with commercial soy flours. *J Appl Polym Sci* 80(1): 10-19.
- Ako M, Kennedy JP (1989) Polyisobutylene-based urethane foams. II. Synthesis and properties of novel polyisobutylene-based flexible polyurethane foams. *J Appl Polym Sci* 37(5): 1351-1361.
- Lligadas G, Ronda JC, Galià M, Cádiz V (2006) Novel Silicon-Containing Polyurethanes from Vegetable Oils as Renewable Resources: Synthesis and Properties. *Biomacromol* 7(8): 2420-2426.
- Guo YS, Ma XY, Wu Z, Zhang SF, Yang XP (2013) Synthesis and Modified of Nonionic Waterborne Polyurethane for Synthetic Leather. *China Leather* 42: 47-57.
- Naghash HJ, Irvani M, Akhtarian R (2014) Synthesis and characterization of monoallyl-end-capped diethylene oxide-based polyurethane surfactant. Synthesis and Reactivity in Inorganic Metal-Organic and Nano-Metal Chemistry 44: 927-934.
- Meiorin C, Mosiewicki MA, Aranguren MI (2013) Ageing of thermosets based on tung oil/styrene/divinylbenzene. *Polymer Testing* 32(2): 249-255.
- Silva VR, Mosiewicki MA, Yoshida MI (2013) Polyurethane foams based on modified tung oil and reinforced with rice husk ash I: Synthesis and physical chemical characterization. *Polymer Testing* 32(2): 438-445.
- Zhang MY, Chen JJ, Yang LC (2011) Research on synthesis and application of anti-wrinkle finishing agent of aliphatic nonionic waterborne polyurethane. *PU Technology* 9: 70-73.
- Zheng J, Luo JX, Zhou DW (2010) Preparation and properties of nonionic polyurethane surfactants. *Colloids Surfaces A: Physicochem Eng Aspects* 363: 16-21.
- Anthemidis AN, Themelis DG, Stratis JA (2001) Stopped-flow injection liquid-liquid extraction spectrophotometric determination of palladium in airborne particulate matter and automobile catalysts. *Talanta* 54(1): 37-43.
- Anthemidis AN, Zachariadis GA, Stratis JA (2002) Online preconcentration and determination of copper, lead and chromium (VI) using unloaded polyurethane foam packed column by flame atomic absorption spectrometry in natural waters and biological samples. *Talanta* 58(5): 831-840.
- Duran A, Tuzen T, Soylak M (2009) Preconcentration of some trace elements via using multiwalled carbon nanotubes as solid phase extraction adsorbent. *J Hazard Mater* 169(1-3): 466-471.
- Soylak M, Tuzen M (2008) Coprecipitation of gold (III), palladium (II) and lead (II) for their flame atomic absorption spectrometric determinations. *J Hazard Mater* 152(2): 656-661.
- Pan L, Qin YR, Hu B, Jiang ZC (2007) Determination of nickel and palladium in environmental samples by low temperature ETWICP-OES coupled with liquid-liquid extraction with dimethylglyoxime as both extractant and chemical modifier. *Chem Res Chin Univ* 23(4): 399-403.
- Candir, S, Narin I, Soylak M (2008) Ligandless cloud point extraction of Cr (III), Pb (II), Cu (II), Ni (II), Bi (III), and Cd (II) ions in environmental samples with tween 80 and flame atomic absorption spectrometric determination. *Talanta* 77(1): 289-293.
- Otero RJ, Moreda PA, Bermejo BA, Bermejo BP (2005) Evaluation of commercial C18 cartridges for trace elements solid phase extraction from seawater followed by inductively coupled plasma optical emission spectrometry determination. *Anal Chim Acta* 536: 213-218.
- Latif, Elci, Aslihan A, Kartal, Mustafa S (2008) Solid phase extraction method for the determination of iron, lead and chromium by atomic absorption spectrometry using Amberite XAD-2000 column in various water samples. *Journal of Hazardous Materials* 153(1-2): 454-461.
- Chen D, Hu B, Huang C (2009) Chitosan modified ordered mesoporous silica as micro-column packing materials for on-line flow injection-inductively coupled plasma optical emission spectrometry determination of trace heavy metals in environmental water samples. *Talanta* 78(3): 491-497.
- Camel V (2003) Solid phase extraction of trace elements. *Spectrochim Acta B at Spectrochim* 58(7): 1177-1233.
- Mohammadi SZ, Afzali D, Pourtalebi D (2011) Flame atomic absorption spectrometric determination of trace amounts of palladium, gold and nickel after cloud point extraction. *J Anal Chem* 66(7): 620-625.
- Bulut Y, Tez Z (2007) Removal of heavy metals from aqueous solution by sawdust adsorption. *J Environ Sci* 19(2): 160-166.
- Li A, Zhang Q, Zhang G, Chen J, Fei Z, et al. (2002) Adsorption of phenolic compounds from aqueous solutions by a water compatible hypercrosslinked polymeric adsorbent. *Chemosphere* 47(9): 981-989.
- Absalan G, Mehrdardi MA (2003) Separation and preconcentration of silver ion using 2-mercaptobenzothiazole immobilized on surfactant-coated alumina. *Purif Technol* 33: 95-101.
- Ensafi AA, Khayamian T, Karbasi MH (2003) Online preconcentration system for lead (II) determination in wastewater by atomic absorption spectrometry using active carbon loaded with pyrogallol red. *Anal Sci* 19(6): 953-956.
- Gupta VK, Ganjali MR, Nayak A, Bhushan B, Agarwal S (2012) Enhanced heavy metals removal and recovery by mesoporous adsorbent prepared from waste rubber tire. *Chem Eng J* 197: 330-342.
- Gupta VK, Ali I, Saleh TA, Nayak A, Agarwal S (2012) Chemical treatment technologies for waste-water recycling-an overview. *RSC Advances* 2(16): 6380-6388.
- Olorundare OF, Krause RWM, Okonkwo JO, Mamba BB (2012) Potential application of activated carbon from maize tassel for the removal of heavy metals in water. *J Phys Chem Earth* 50-52:104-110.

28. Ferri T, Sangiorgio P (1996) Determination of selenium speciation in river waters by adsorption of iron (III)-chelex-100 resin and differential pulse cathodic stripping voltammetry. *Anal Chim Acta* 321(2-3): 185-193.
29. Pinto ML, Pires J, Carvalho AP, Carvalho MB, Bordado, JC (2004) Synthesis and characterization of polyurethane foam matrices for the support of granular adsorbent materials. *J Appl Polym Sci* 92: 2045.
30. Akl MA, Kenawy IMM, Lasheen RR (2004) Organically modified silica gel and flame atomic absorption spectrometry: employment for separation and preconcentration of nine trace heavy metals for their determination in natural aqueous systems. *Microchem J* 78: 143-156.
31. Gupta VK, Nayak A (2012) Cadmium removal and recovery from aqueous solutions by novel adsorbents prepared from orange peel and Fe<sub>2</sub>O<sub>3</sub> nanoparticles. *Chem Eng J* 180: 81-90.
32. Sanghavi BJ, Mobin SM, Mathur P, Lahiri GK, Srivastava AK (2013) Biomimetic sensor for certain catecholamines employing copper (II) complex and silver nanoparticle modified glassy carbon paste electrode. *Biosens Bioelectron* 39(1): 124-132.
33. Krause RWM, Mamba BB, Bambo FM, Malefetsa TJ (2010) Cyclodextrin polymers: synthesis and application in water treatment. In: Hu J (ed) *Cyclodextrins: chemistry and physics*, vol 9. Transworld Research Network, Kerala, pp 185-208.
34. Ngah WS, Teong LC, Toh RH, Hanafiah MAKM (2012) Utilization of chitosan-zeolite composite in the removal of Cu (II) from aqueous solution: adsorption, desorption and fixed bed column studies. *Chem Eng J* 209: 46-53.
35. Kiliaris P, Papispyrides CD (2010) Polymer/layered silicate (clay) nanocomposites: an overview of flame retardancy. *Prog Polym Sci* 35(7): 902-958.
36. Saghia M, Kavianib D, Bagheric Z, Padidarand B, Bigtana MH, et al. (2015) Removal of copper ions from contaminated aqueous solutions through adsorption process using modified polyurethane (PU) as an adsorbent. *Scientific Journal of Environmental Sciences* 4(4) 97-101.
37. Olorundare OF, Msagati TA, Krause RWM, Okonkwo JO, Mam BB (2014) Polyurethane composite adsorbent using solid phase extraction method for preconcentration of metal ion from aqueous solution. *Int J Environ Sci Technol* 12(7): 2389-2400.
38. Shokry SA, El Morsi AK, Sabaa MS, Mohamed RR, El Sorogy HE (2015) Synthesis and characterization of polyurethane based on hydroxyl terminated polybutadiene and reinforced by carbon nanotubes. *Egypt J Petrol* 24(2): 145-154.
39. Puigdomenech, Hydra I (hydrochemical equilibrium-constant database) and MEDUSA (make equilibrium diagrams using sophisticated algorithms) programs, Royal Institute of Technology, Sweden.
40. Marczenko Z (1976) *Spectrophotometric Determination of the Elements*, John Wiley, London, Uk.
41. Sheng L, Zhou L, Huang Z, Liu Z, Chen Q, et al. (2016). Facile synthesis of magnetic chitosan nanoparticles functionalized with NO-containing groups for efficient adsorption of U(VI) from aqueous solution *J Radioanal Nucl Chem* 310: 1361-1371.
42. Li L, Ding D, Hu N, Fu P, Xin X, Wang Y (2014) Adsorption of U(VI) ions from low concentration uranium solution by thermally activated sodium feldspar. *J Radioanal Nucl Chem* 299: 681-690.
43. Manes M, Hofer LJE (1969) Application of the Polanyi adsorption potential theory to adsorption from solution on activated carbon, *The Journal of Physical Chemistry* 73(3): 584-590.
44. Abderrahim O, Didi MA, Villemin D (2009) A new sorbent for uranium extraction polyethyleneimine phenyl phosphonamic acid. *J Radioanal Nucl Chem* 279(1): 237-244.
45. Ansari SA, Mohapatra PK, Manchanda VK (2009) A novel malonamide grafted polystyrene- divinyl benzene resin for extraction pre-concentration and separation of actinides, *J Hazard Mater* 161(2-3): 1323-1329.
46. Metilda P, Sanghamitra K, Mary GJ, Naidu GRK, Prasada RT (2005) Amberlite XAD-4 functionalized with succinic acid for the solid phase extractive preconcentration and separation of uranium (VI). *Talanta* 65(1): 192-200.
47. Venkatesan K, Sukumaran V, Antony MP, Vasudeva RPR (2004) Extraction of uranium by amine, amide and benzamide grafted covalently on silica gel, *J Radioanal Nucl Chem* 260(3): 443-450.
48. Camacho LM, Deng S, Parra RR (2010) Uranium removal from groundwater by natural clinoptilolite zeolite: effects of pH and initial feed concentration. *J Hazard Mater* 175(1-3): 393-398.
49. Ferrah N, Abderrahim O, Didi MA (2015) Comparative Study of Cd<sup>2+</sup> Ions Sorption by Both Lewatit TP214 and Lewatit TP 208 Resins: Kinetic, Equilibrium and Thermodynamic Modelling, *Chemistry Journal* 5(1): 6-13.
50. Cheira MF (2015) Synthesis of pyridylazo resorcinol – functionalized Amberlite XAD-16 and its characteristics for uranium recovery. *Journal of Environmental Chemical Engineering* 3(2): 642-652.
51. Shabaan, Salah M, Daher, Ahmed M, Hussein AEM, et al. (2018) Uranium Adsorption from Aqueous Solution by Trioctylamine Impregnated Polyurethane Foam. *J Chem Bio Phys Sci Sec C* 8(4): 368-385.
52. Lagergren S (1898) Zur theorie der sogenannten adsorption gelöster stoffe *Kungliga venska Vetenskapsakademiens. Handlingar* 24(4): 1-39.
53. Ho YS, McKay G (1999) Pseudo-second order model for sorption processes, *Process Biochem* 34(5): 451- 465.



This work is licensed under Creative Commons Attribution 4.0 License  
DOI: [10.19080/AJOP.2019.03.555604](https://doi.org/10.19080/AJOP.2019.03.555604)

### Your next submission with Juniper Publishers will reach you the below assets

- Quality Editorial service
- Swift Peer Review
- Reprints availability
- E-prints Service
- Manuscript Podcast for convenient understanding
- Global attainment for your research
- Manuscript accessibility in different formats  
**( Pdf, E-pub, Full Text, Audio )**
- Unceasing customer service

**Track the below URL for one-step submission**  
<https://juniperpublishers.com/online-submission.php>